The influences of historic lake trophy and mixing regime changes on long-term phosphorus fractions retention in sediments of deep, eutrophic lakes: a case study from Lake Burgäschi, Switzerland

Luyao Tu[1], Paul Zander[1], Sönke Szidat[2], Ronald Lloren[3,4], Martin Grosjean[1]

1 Oeschger Centre for Climate Change Research and Institute of Geography, University of Bern, Switzerland

2 Oeschger Centre for Climate Change Research and Department of Chemistry and Biochemistry, University of Bern, Switzerland

3 Department of Earth Science, ETH Zürich, Switzerland

4 Eawag, Swiss Federal Institute of Aquatic Science and Technology, Switzerland

Correspondence to: Luyao Tu (luyao.tu@giub.unibe.ch)

Abstract. Hypolimnetic anoxia in eutrophic lakes can delay lake recovery to lower trophic states via the release of sediment phosphorus (P) to surface waters on short time scales in shallow lakes. However, the long-term effects of hypolimnetic redox conditions and trophic state on sedimentary P-fraction retention in deep lakes are not clear yet. Hypolimnetic withdrawal of P-rich water is predicted to diminish sedimentary P and seasonal P recycling from the lake hypolimnion. Nevertheless, there is a lack of evidence from well-dated sediment cores, in particular, from deep lakes, about the long-term impact of hypolimnetic withdrawal on sedimentary P retention. In this study, long-term sedimentary P-fraction data since the early 1900s from Lake Burgäschi provides information on the benthic P retention under the influence of increasing lake primary productivity (sedimentary green-pigments proxy), variable hypolimnion oxygenation regimes (Fe/Mn ratio proxy), and hypolimnetic withdrawal since 1977. Results show that, before hypolimnetic withdrawal (during the early 1900s to 1977), redox-sensitive Fe/Mn-P fraction comprised ~50% of total P in the sediment profile. Meanwhile, long-term retention of total P and labile P-fractions in sediments was predominantly affected by past hypolimnetic redox conditions, and P retention increased in sedimentary Fe- and Mn enriched layers when the sediment overlaying water was seasonally oxic. However, from 1977-2017, eutrophication-induced persistent anoxic conditions in the hypolimnion and due to hypolimnetic water withdrawal increasing the P export out of the lake, net burial rates of total and labile P fractions decreased considerably in surface sediments. By contrast, refractory Ca-P fraction retention was primarily related to lake primary production. Due to the lake restoration since 1977, Ca-P fraction became the primary P fraction in sediments (representing ~39% of total P), indicating a lower P bioavailability of surface sediments. Our study implies that in seasonally-stratified eutrophic deep lakes (like Lake Burgäschi), hypolimnetic withdrawal can effectively reduce P retention in sediments and potentials of sediment-P release (internal P loads). However, more than 40 years of hypolimnetic syphoning have not improved the lake trophic state or decreased lake productivity. Also, this restoration has not enhanced water-column mixing and oxygenation in hypolimnetic waters. The findings of this study are relevant regarding management of deep eutrophic lakes with mixing regimes typical for temperate zones.

Keywords: Phosphorus fractions, eutrophication, hypolimnetic anoxia, hypolimnetic withdrawal, deep lakes

39

1 Introduction

Phosphorus (P) eutrophication in freshwater lakes is a global problem and has been a matter of concern to the public for several decades. In lakes where the external P loading has been reduced, internal P loading (sediment-P release to surface waters) is widely recognized as the key factor affecting lake trophic status and delaying lake recovery from eutrophication (Burley et al., 2001; Trolle et al., 2010). Considerable work has been done on sediment-P speciation to evaluate sediment-P release potentials and implications for lake restoration management (Gonsiorczyk et al., 1998; Ribeiro et al., 2008).

The paradigm that oxygen levels control the sediment-P release via reductive dissolution of Fe-P fraction in surface sediments has been accepted as the classical model for a long time (Einsele, 1936, 1938; Moosmann et al., 2006). Under anoxic conditions, P bound to redox-sensitive Fe and Al/Fe (oxyhydr)oxides can be potentially released from surface sediments into lake water (Burley et al., 2001), which was supported by numerous short-term (days or seasonal) laboratory or in-situ studies (Chen et al., 2018). Based on this paradigm, it was assumed that an oxic sediment–water interface might limit the release of Fe-P from sediments and, therefore, improve P retention in lake sediments. However, the restoration measures with artificial hypolimnetic oxygenation/aeration applied in eutrophic lakes proved to have only short-lasting effects but no direct effects on internal P loading and redox-dependent sediment-P retention on longer terms (Gächter, 1987; Gächter and Wehrli, 1998; Moosmann et al., 2006; Hupfer and Lewandowski, 2008). Gächter and Müller (2003) and Moosmann et al. (2006) further argued that, on multi-decadal or longer time scales, P retention in lake sediments might eventually primarily depend on the P-binding capacity of anoxic sediments and sediment composition (e.g. Fe, Mn, Al, and Ca contents). Nevertheless, until now, there is a lack of evidence from well-dated sediment cores, and there is still a need to know which processes may have a dominant influence on sediment P-fraction retention on longer time scales (e.g., decades or more). This information is crucial for predicting and, ultimately, managing sediment-P release, especially in deep lakes, because hypolimnetic anoxia in deep lakes can lead to large loads of sediment-P release. In contrast to the well-established studies about sediment-P speciation in shallow polymictic lakes (e.g. Kaiserli et al., 2001; Søndergaard et al., 2001; Cavalcante et al., 2008), there are only a few studies available from seasonally-stratified deep lakes. Furthermore, eutrophication has been demonstrated to affect sediment-P release via controlling hypolimnetic anoxia and lake mixing regime in seasonally stratified deep lakes (Tu et al., 2019). It is not yet fully understood whether and how lake trophic levels and hypolimnetic anoxia can influence the long-term behavior of sedimentary P-fraction retention in deep lakes.

The restoration technique of hypolimnetic withdrawal has been frequently applied in seasonally stratified lakes in Europe (Kucklentz and Hamm, 1988; Nürnberg, 2007), whereby P-enriched water from the hypolimnion is discharged directly into the lake outflow. This restoration technique has been shown to efficiently reduce P concentrations in lake waters (Nürnberg, 2007). Hypolimnetic withdrawal was also expected to reduce P retention in sediments and seasonal P recycling from the lake hypolimnion to the upper waters, for example, in Lake Mauen, a shallow, eutrophic lake (maximum depth 6.8 m; Gächter, 1976). However, there is lack of empirical evidence from sedimentary P-fraction data, which provides valuable information on possible sediment-P release

76 characteristics and potentials of internal P loadings. Furthermore, for deep lakes, the long-term influence of this

77 restoration on sedimentary P release potentials is unclear.

78 The objectives of this study were to (1) explore the main factors controlling long-term changes of P-fraction

79 retention in sediments of deep lakes, (2) investigate how sediment P-fraction retention responds to changes in lake

80 eutrophication and hypolimnetic anoxia of the past prior to anthropogenic eutrophication, (3) examine the long-

81 term effects of lake hypolimnetic withdrawal restoration on sedimentary P-fraction retention in seasonally-

82 stratified deep lakes, and (4) evaluate with sediment-P data the predictions from Gächter (1976) that hypolimnetic

83 withdrawal should result in reduced total P contents in sediments and sediment-P release to lake water. To achieve

84 these objectives, we investigated short sediment cores from Lake Burgäschi, a deep and eutrophic lake on the

85 Swiss Plateau. Sedimentary green-pigments (chlorophylls and diagenetic products) inferred from hyperspectral

86 imaging (HSI) scanning and XRF-inferred Fe/Mn ratios primarily reflect lake trophic state evolution (aquatic

87 primary productivity) and hypolimnetic oxygenation, respectively. A sequential P-extraction with five P fractions

88 was performed to uncover P fractionation in sediment profiles. We combined all data to identify the dominant

89 factors responsible for temporal changes in P-fraction retention.

90 Lake Burgäschi is an excellent study site because there were substantial changes in lake trophic levels and possibly

91 lake-mixing regimes since the last century (Guthruf et al., 1999; Van Raden, 2012), and exceptionally long

92 historical and limnological survey data are available for most of the last 50 years. Hypolimnetic withdrawal

93 restoration is in operation since 1977.

94

95 **2 Study site**

96 Lake Burgäschi (47°10′8.5″N, 7°40′5.9″E) is a small lake located on the Swiss Plateau (Fig. 1a). It has a very

97 restricted catchment (3.2 km²). The catchment area geologically belongs to the Molasse Basin, and mostly consists

98 of carbonate-rich sandstones and mudstones (Schmid et al., 2004). The kettle hole lake was formed after the retreat

99 of the Rhone glacier (ca. 19 k yr. BP; Rey et al., 2017). Currently the maximum water depth is ~31 m, which is

100 quite deep in contrast to the small surface area of 0.21 km² (Guthruf et al., 1999). The mean retention time of the

101 lake water is ~1.4 year (Nürnberg, 1987). The lake has several small inflows in the southwest (Rey et al., 2017)

102 and one outflow in the north (Fig. 1c).

103 Since the 19th century, the lake's water level was lowered several times to create farmland, with the most recent

104 lowering (up to 2 m) during 1943-1945 (Guthruf et al., 1999). Agricultural area currently covers ~55% of the lake

105 catchment, followed by ~29% area of forests. The lake region experiences a warm humid continental climate (Dfb;

106 Köppen-Geiger classification). The mean annual air temperature is 9 °C and the warmest month is July (mean

107 temperature 19 °C).

108 Lake Burgäschi has been highly productive (eutrophic to highly eutrophic state) since the 1970s with high algal-

109 biomass production and anoxic conditions in the hypolimnion (Guthruf et al., 1999, 2013). The eutrophication in

110 Lake Burgäschi has been linked to increased agricultural P inputs via drainage into the lake in the second half of

111 the 20th century (Guthruf et al., 1999). To mitigate the eutrophication, hypolimnetic withdrawal restoration has

112 been applied in Lake Burgäschi since 1977, and the lake water has been monitored twice a year for more than 30

113 years for various parameters, such as pH, oxygen content, phosphorus concentrations, phytoplankton biomass, etc.
114 Despite a sharp decline in hypolimnetic phosphorus concentrations due to the restoration, a high production of
115 algal biomass continues today (GSA, 2007). Additionally, hypolimnetic oxic/anoxic conditions and the lake
116 trophic state have been stabilized but not fundamentally improved (GBL, 1995; Guthruf et al., 2013).

117

3 Materials and methods

3.1 Core collection and sampling

120 In September 2017, two 75-cm-long sediment cores (Burg17-B and Burg17-C) were retrieved from the deepest
121 point of Lake Burgäschi (water depth ~31 m) (47°10'8.6"N, 07°40'5.3"E; coring site in Fig. 1c) using a UWITEC
122 gravity corer. After the collection, the cores were stored in a dark cold room (~4 °C). After opening and splitting
123 lengthwise, core-half A of Burg17-B was continuously subsampled at 2-cm resolution from 0 to 60 cm for ^{210}Pb
124 and ^{137}Cs dating. The oxidized surface of core-half B (Burg17-B) was visually described (Schnurrenberger et al.,
125 2003) before non-destructive XRF core and HSI scanning. After the opening, one-half of core Burg17-C was
126 transferred immediately into a glove box with an anoxic atmosphere where it was continuously subsampled at 2-
127 cm resolution from 0 to 72 cm. The fresh sediments from each sample slice were homogenized and used for
128 sequential P extraction. After sampling for P extraction, the remaining sediment of the 2-cm slice was freeze-dried
129 and homogenized for bulk element analyses.

3.2 Chronology

131 The chronology of the core Burg17-B is based on ^{210}Pb and ^{137}Cs activity profiles. The freeze-dried and
132 homogeneous samples were stored dry and dark until analysis. The ^{210}Pb, ^{137}Cs and ^{226}Ra radiometric activities
133 were measured by gamma spectrometry at the University of Bern Department of Chemistry and Biochemistry.
134 1.3-5.1 g of the freeze-dried samples were encapsulated into polystyrene petri dishes (68 mm O.D., 11 mm height;
135 Semadeni, Ostermundigen, Switzerland) together with a polystyrene disk to fill in the headspace above the sample
136 material, and the petri dishes were vacuum-sealed into a gas-tight aluminum foil for equilibration. ^{210}Pb (46.5 keV),
137 ^{241}Am (59.5 keV), ^{226}Ra progenies ^{214}Pb and ^{214}Bi (295.2, 351.9 and 609.3 keV), as well as ^{137}Cs (661.7 keV) were
138 measured using a Broad Energy Germanium (BEGe) detector (Canberra GmbH, Rüsselsheim, Germany). This
139 system is composed of a high-purity germanium crystal of 50 cm^2 area and 30 mm thickness with a 0.6 mm thick
140 carbon epoxy window, which shows high absolute full-energy peak efficiencies for close on-top geometries of >20%
141 and ~5% for ^{210}Pb and ^{137}Cs, respectively. Low integrated background count rates of 0.20 s^{-1} (energy range of 30-
142 1800 keV) were achieved by application of low-background materials, installation in third underground floor (~10
143 m of water-equivalent overburden), passive shielding (outside to inside: 10 cm low-background lead, 3 mm ancient
144 lead with negligible ^{210}Pb content, 2 mm cadmium), flushing of the shield interior with nitrogen gas and an active
145 anti-cosmic shield (plastic scintillator panels of totally 1 m^2 area mounted directly above the passive shielding).
146 Supported ^{210}Pb in each sample was assumed to be in equilibrium with the in-situ ^{226}Ra (equilibration time 4
147 weeks). Unsupported ^{210}Pb activity was calculated by subtracting ^{226}Ra activity from total ^{210}Pb activity level-by-
148 level. The correction for the total unsupported ^{210}Pb missing inventory followed Tylmann et al. (2016).

149

The ^{210}Pb chronology of core Burg17-B was determined using the Constant Rate of Supply (CRS) model (Appleby, 2002), which accounts for variation in sediment accumulation rates. We tested two CRS models: CRS-1 model was unconstrained (i.e. without reference points from the ^{137}Cs activity). The CRS-2 model was constrained with the chronologic marker of peak fallout from nuclear weapons testing in 1963 (^{137}Cs and ^{241}Am). Both models were then tested and validated with independent time-markers at the onset of nuclear weapons testing in 1953/54 and the Chernobyl accident in 1986/87 (onset of ^{137}Cs and peak of ^{137}Cs and ^{241}Am, respectively).

The two sediment cores (Burg 17-B and Burg 17-C) are visually very similar but show a length-offset due to coring compaction of approximately 2-6 cm (Fig. S1 in Supplementary data). The age-depth stratigraphy of Burg17-C core was inferred from the dated core Burg17-B by visual stratigraphic correlation from high-resolution core pictures.

3.3 Non-destructive geochemical methods

Non-destructive X-ray fluorescence (XRF) core scanning was done using an Avaatech XRF Core Scanner (Richter et al., 2006) for semi-quantitative element composition measurements at 0.5 mm resolution to capture relative elemental concentrations of the laminae. The core surface was smoothed and covered with a 4-μm-thick Ultralene foil prior to the analysis. Elements were measured using a Rhodium anode and a 25 μm Be window. The lighter elements (e.g. Al, Si, P etc.) were measured for 15 seconds count time at 10 kV with 1500 A, no filter; while the heavier elements (e.g. Mn, Fe, Br etc.) were exposed for 40 seconds at 30 kV with 2000 A, Pd-thin filter. Element intensities (semi-quantitative concentrations) of the selected elements (Mg, Si, Al, K, Ti, Rb, P, Fe, Mn, Ca) are expressed as count rates (counts per second, cps).

Following the methodology in Butz et al. (2015), hyperspectral imaging (HSI) scanning was performed using a Specim Ltd. Single Core Scanner equipped with a visual to near infrared range (VNIR, 400–1000 nm) hyperspectral linescan camera (Specim PFD-CL-65-V10E). Parameters were set for a spatial resolution of ~70 μm/pixel and a spectral sampling of 1.57 nm (binning of 2). Spectral endmembers were determined using the "Spectral Hourglass Wizard" of the ENVI 5.5 software package (Exelisvis ENVI, Boulder, Colorado). The relative absorption band depth (RABD) index calculation was performed following the method in Schneider et al. (2018). However, based on the spectral end members (Fig. S2), we used the absorption feature between the wavelengths R590 and R765 (590-765 nm), i.e. RABD$_{590-765}$. Butz et al. (2017) and Schneider et al. (2018) revealed that this index is well calibrated to absolute green-pigments (chlorophyll *a* + pheophytin a) concentrations in sediments. The sediments in Lake Burgäschi are mostly laminated and organic-rich (Van Raden, 2012), which indicates that the sediments are anoxic, bioturbation is absent, and sedimentary pigments are well-preserved (Reuss et al., 2005). Therefore, in our study, the relative concentrations of green-pigments inferred from RABD$_{590-765}$ index values provide a semi-quantitative reconstruction of lake primary productivity (total algal abundance) at sub-annual resolution, and are suggested to reflect the trophic state evolution of Lake Burgäschi.

3.4 Phosphorus fractionation scheme and bulk elements analyses

The P-fractionation extraction protocol (Fig. S3) principally follows the four-step extraction protocol in Tu et al., (2019). In addition, we added the last extraction step from Lukkari et al. (2007) to determine refractory organic P

(F5). This P fraction (F5) is practically biologically unavailable and subject to permanent P burial. The first four fractions are NaCl-TP (F1: loosely bound P), NaBD-TP (F2: redox-sensitive Fe- and Mn-bound P), NaOH-TP (F3: Al- and Fe-bound P), and HCl-TP (F4: Ca-bound P) (Tu et al., 2019), whereby NaCl-TP, NaBD-TP and NaOH-TP fractions together are considered as relatively labile P fractions because they may release P back to the water column under anoxic or high pH environments (Rydin, 2000). The HCl-TP and refractory organic P (Ref.-P_o) fractions are classified as relatively stable or refractory P fractions. Total P in sediments was obtained from the sum of the five P fractions. The P in extract samples was measured by inductively coupled plasma mass spectroscopy (7700× ICP-MS) (Agilent Technologies, Germany) after the dilution with nitric acid (HNO_3) to reach a final concentration of 1% v/v HNO_3.

Concentrations of total carbon (TC), total nitrogen (TN), and total sulfur (S) in sediment samples were determined using an Elementar vario EL Cube elemental analyzer. Total inorganic carbon (TIC) content was calculated by multiplying loss on ignition at 950 °C (LOI_{950}, following the method proposed by Heiri et al. (2001)) by 0.273, i.e. the ratio of the molecular weight of C and CO_2. Total organic carbon (TOC) content was calculated using the equation TOC =TC-TIC. Sediment dry bulk density and water content were determined using wet mass (g), dry mass (g) and wet volume (cm^3) following the method in Håkanson and Jansson (2002).

3.5 Data analyses

Multivariate statistical analyses were performed with R version 3.4.2 (R Development Core Team, 2017). Prior to data analyses, $RABD_{590-765}$ index values (resolution 70 μm) were aggregated to a spatial resolution of 0.5 mm (the spatial resolution of XRF data). Stratigraphically constrained incremental sum of squares clustering (CONISS; Grimm, 1987) was then performed on semi-quantitative proxies (i.e. $RADB_{590–765}$ index and XRF-element data) with R-package ''rioja'' (Juggins, 2017). The number of significant clusters was determined with a broken-stick test (Bennett, 1996). A principal components analysis (PCA) was performed on the centered and standardized data of semi-quantitative proxies, using the "Vegan" package (Oksanen et al., 2013). XRF-element and $RABD_{590-765}$ index values were averaged within the depth range of each sample taken from core Burg17-C for P fractions. In order to identify the primary factors influencing the variations in sedimentary P fractions, a redundancy analysis (RDA) was performed on the centered and standardized dataset of P fractions (response variables) and other sediment geochemical parameters (explanatory variables) with the "vegan" package. In the RDA computation, the correlation matrix option was selected and the scaling was conducted on a correlation biplot.

4 Results

4.1 ^{137}Cs and ^{210}Pb chronology

The two distinctive peaks of ^{137}Cs in sediment profiles are detected at 31 cm and 15 cm depths (Fig. 2b), corresponding to the 1963 and 1986 major fallout events, respectively (Appleby, 2002). Furthermore, [241]Am activity peaks at the same depths (Fig. 2b) confirm that the 1963 and 1986 ^{137}Cs peaks were due to atmospheric fallouts (Michel et al., 2001). The first traces of ^{137}Cs occur at 37 cm depth, indicating the first widely detectable fallout from atmospheric nuclear testing in 1953/1954 (Pennington et al., 1973).

224 The ^{210}Pb activity in core Burg17-B shows a relatively monotonic decrease down to a sediment depth of 17 cm.
225 Further down, larger variations are found (Fig. 2a). The ^{210}Pb and ^{226}Ra activities do not reach equilibrium;
226 unsupported ^{210}Pb activity in the oldest sample (59 cm) is still above the limit of detection (14.0±6.8 Bq·kg^{-1}). The
227 observed cumulative inventory of unsupported ^{210}Pb is 2941 Bq·m^{-2}. We corrected this value (missing inventory
228 correction; Tylmann et al., 2016) by applying an exponential equation using the lowermost values of cumulative
229 dry mass and unsupported ^{210}Pb activity between 8 and 60 cm depths. As a result, a correction value of 125.2
230 Bq·m^{-2} (missing inventory) is added to the final total unsupported ^{210}Pb inventory (3066 Bq·m^{-2}).

231 The CRS-2 model (constrained through 1963) shows a better agreement with the independent ^{137}Cs markers at
232 1953/54 and 1986/87 than the CRS-1 model (Fig. 2c). Therefore, CRS-2 model results were chosen for determining
233 the age-depth profile and sediment mass accumulation rates (MAR) of core Burg17-B. The mean age at 59 cm
234 sediment depth dates back to ~1930. The extrapolated mean age at 61 cm depth is ~1926 calculated using the mean
235 sediment accumulation rate between 54-60 cm (2 yr·cm^{-1}).

236 **4.2 Sediment lithology, green-pigments (RABD$_{590-765}$ index) and XRF-element records**

237 Four sediment facies (I to IV, Fig. 3 and 4a) are identified based on visual classification and the CONISS-analysis
238 results of XRF-element intensities.
239
240 In Zone I (75.4-61cm, pre ~1926), the sediments consist of visible thin brown-to-reddish laminae (Mn- and Fe
241 rich). Green-pigment concentrations inferred from RABD$_{590-765}$ index values show a homogenous distribution with
242 the lowest values within the sediment profile (Fig. 4d). Fe/Mn ratios vary within very low values (mostly below
243 10). The Mn, Fe, P and Fe/Ti values show high levels with large variability. Extremely low Ca amounts are noted
244 in this zone.
245
246 In Zone II (61-34cm, ~1926-1960), the sediments are dark gyttja, partly laminated with light Ca-rich layers. Green-
247 pigment concentrations slightly increase yet still show little variability. A sharp increase of green-pigments
248 concentrations occurs at 60 cm, and the first two local peaks near 55 cm (~1938) and 48 cm (1945) are notable.
249 Fe/Mn ratios remain at slightly higher values than in Zone I. The Mn, Fe, P contents and Fe/Ti values all decline
250 to low levels and remain relatively stable. Ca counts increase gradually over the whole Zone II.
251
252 In Zone III (34-21.5 cm, ~1960-1977), the sediments are mostly characterized by brown-to-reddish laminations
253 (Mn-Fe rich), with thicker and more distinct laminae contacts than in Zone I. Green-pigment concentrations exhibit
254 much higher values with positive trends, intensified variability, and several maxima (seasonal algal blooms).
255 Fe/Mn ratios first drop in the lower part (34-27 cm) and then continue to increase upward to the top-part of Zone
256 III. Fe, Mn, P, and Fe/Ti values show generally opposing trends to Fe/Mn ratios. Ca contents are elevated during
257 this period relative to Zones I and II.
258
259 In Zone IV (21.5-0 cm, ~1977-2017), the sediments exhibit a clear laminated structure with much more
260 pronounced light calcite layers. The laminations are characterized by a regular succession of light calcite layers
261 (Ca-rich) and dark organic-rich layers (Fig. S4). Green-pigment concentrations display the highest levels with
262 large fluctuations, and reach distinct local maxima at 18 cm (1981), 15 cm (1985), 13 cm (1987), 12 cm (1988),

263 and 8 cm (1997) depths (Fig. 4d). Fe/Mn ratios are at similarly high values as in Zone II, yet with more variability.
264 The Fe, Mn, and P element counts and Fe/Ti all show constantly very low values. The Ca amounts are the highest
265 in the profile and show considerable variability.

266

267 Two principle components, PC1 and PC2 were shown to be significant using a broken stick model. They explain
268 ~35 % and ~30 % of the total variance in the dataset, respectively (PCA-biplot; Fig. S5). The PC1 has strong
269 positive loadings for the terrigenous elements (K, Ti, Rb etc.; Fig. 3 and S6) and thus represents mainly erosional
270 processes related to allochthonous inputs. The PC2 has strong positive loadings for redox-sensitive elements (Fe,
271 Mn), P and Fe/Ti, but negative loadings for Ca, Fe/Mn ratios and green-pigments index values. Therefore, PC2
272 reflects changes in redox conditions of hypolimnetic water and lake primary productivity. The results of additional
273 PCA analyses zone by zone (Fig. S7b) show that Mn, Fe and P were mostly independent of terrigenous elements
274 (in Zones I to III), however in Zone IV, Mn, Fe and P become correlated with the terrigenous elements. The vertical
275 profile of XRF-P matches very well with the changes of total P concentrations in sediments (Fig. S8). It reveals
276 that XRF-P data can reliably represent qualitative variations of total P concentrations in sediment profiles of Lake
277 Burgäschi.

278

279 **4.3 Bulk elements and P fractions in sediment profiles**

280 Sediment TIC, TOC, TOC/TN ratio, S and P fractions also show distinctive features along the four stratigraphic
281 zones (Fig. 5). From the upper part of Zone I (65.2-61 cm; ~1926) to Zone IV, TIC shows a similar pattern to the
282 XRF-Ca contents (Fig. 3 and 5) suggesting that TIC is mostly present in the form of $CaCO_3$. Over the whole profile,
283 TOC/TN ratios are within the range of 9-11. TOC and TOC/TN ratios exhibit mostly similar patterns from Zone I
284 to Zone III. By contrast, total sulfur (S) contents display a different pattern, showing very low values in Zone I
285 and II (mean ~0.5%), and a substantial increase in Zone III and IV.

286

287 The concentrations of labile P fractions (i.e. NaCl-TP, NaBD-TP and NaOH-TP) and total P have a similar trend
288 over the whole profile (Fig. 5 and 6a). They all display rather large values within the upper part of Zone I and
289 generally decreased values in Zone II. In Zone III, the values increase to peaks at ~25 cm depth but sharply decrease
290 to the lowest values in the upper boundary of Zone III and throughout Zone IV. HCl-TP and Ref.-P_o fractions vary
291 differently compared with the other fractions. Low contents of HCl-TP fraction are observed in Zone I and II. HCl-
292 TP fraction has a rather similar pattern as labile P fractions in Zone III, but then it remains at high levels in Zone
293 IV. Ref.-P_o fraction contents show relatively stable values from Zone I to Zone II, followed by a gradual rise in
294 Zone III and in the upper part of Zone IV. The net burial rates (NBR) of P-fraction since 1934 (Fig. S9) show
295 similar trends to the P-fraction concentrations (Fig. 5) (because sedimentation rates MAR are rather constant in
296 core Burg17-C; Fig S9), except for the Ca-P and Ref.-P_o fractions with decreasing NBR throughout the Zone IV.

297

298 Regarding the P composition in sediment profiles (Fig. 6, absolute and relative amounts), from Zone I to Zone III
299 (65.2-21.5 cm) NaBD-TP fraction is the most important P-form representing ~50% of total P followed by NaOH-
300 TP fraction. However, in Zone IV (depth above ~ 21.5 cm), HCl-TP becomes the main P fraction (~39% of total
301 P) over NaBD-TP (~30% of total P).

302

303   The relationships between response variables and explanatory variables are visible on the redundancy analysis
304   (RDA) biplot (Fig. 7), which, in most cases, correspond well to the results of Spearman rank correlation test (Fig.
305   S10). The relatively labile P fractions (NaCl-TP, NaBD-TP and NaOH-TP) and total P in sediments are strongly
306   positively correlated with redox-sensitive elements (Fe and Mn) and autochthonous Fe (Fe/Ti). However, these P
307   fractions are negatively related to hypolimnetic oxygenation proxy (Fe/Mn ratios) and, to some extent, to lake
308   productivity indicators (green-pigments, XRF-Ca and TIC). HCl-TP and Ref.-P_o fractions are positively correlated.
309   However, only HCl-TP fraction has close positive relationships with lake productivity indicators.

310   **5 Discussion**

311   **5.1 Trophic state evolution of Lake Burgäschi**

312   Four main phases of different lake trophic levels (based on $RABD_{590-765}$ index values) were distinguished since the
313   early 1900s, as summarized in Fig. 8 and Fig. S11. During the period prior to ~1926 in Zone I, the lowest green-
314   pigments index values reflect low lake primary productivity. In the early 1900s, agricultural impacts around the
315   catchment area of Lake Burgäschi were not prominent (Guthruf et al., 1999). It can be expected that the lake
316   received low nutrient loads from the catchment drainage during this period. Lake Burgäschi is classified as
317   naturally oligotrophic based on morphometric parameters (LAWA, 1998) and as naturally mesotrophic according
318   to Binderheim-Bankay (1998). Therefore, at the times of Zone I, Lake Burgäschi was likely oligo- to mesotrophic.
319

320   The transition to Zone II (~1926-1960) was marked by generally increased sedimentary green-pigment
321   concentrations and $CaCO_3$ contents (Fig. 3, 4d and 5), respectively, indicating enhanced lake primary productivity.
322   The slightly decreased TOC/TN ratio also suggests a rise in autochthonous organic matter proportion (Meyers and
323   Ishiwatari, 1993). The first two algal blooms (peaks of green-pigments index; Fig. 4d) imply a very likely
324   mesotrophic to eutrophic state of the lake. Indeed, the study of Büren (1949) revealed that in 1943-1945, the trophic
325   state of Lake Burgäschi had already shifted between mesotrophic and eutrophic. Interestingly, the water-table
326   lowering during 1943-1945 (Guthruff et al., 1999) with related enhanced drainage of intensive agricultural fields
327   and meadows (Büren, 1949) did not seem to have had an immediate impact on lake primary productivity (Fig. 3).
328

329   In Zone III (~1960-1977), continuously increasing green-pigment concentrations indicating several algal bloom
330   events and intensified $CaCO_3$ precipitation (TIC) and sulfur (S) contents in sediments (Fig. 4a and 5) are in
331   agreement with the findings from other eutrophic lakes (Holmer and Storkholm, 2001; Bonk et al., 2016; Schneider
332   et al., 2018).
333

334   During Zone IV (1977-2017), we interpret that Lake Burgäschi was in highly eutrophic conditions, based on
335   constantly high green-pigments index values and multiple prominent algal blooms (Fig. 3). Low and decreasing
336   TOC/TN ratio values (< 10) in this zone suggest a dominant source of organic matter in sediments from aquatic
337   primary production, which has been interpreted as a signal of eutrophic waters (Enters et al., 2006). Our
338   interpretation is further supported by high chlorophyll-*a* concentrations in surface waters (>8 ug L^{-1}; GSA, 2007)

and the dominance of blue-green algae in the phytoplankton biomass during 1977 to 1992, which characterized Lake Burgäschi as highly eutrophic (GBL, 1995; Guthruf et al., 2013).

5.2 Reconstruction of hypolimnetic oxygenation regimes of Lake Burgäschi

A large number of studies have used the proxy of Fe/Mn ratios in sediments to reconstruct past water oxygenation and mixing regimes of the lake, such as Mackereth (1966), Frugone-Álvarez et al. (2017), and Żarczyński et al. (2019) etc. However, this proxy and its interpretation are limited to cases in which the annual cycle of Fe and Mn deposition in lakes is mostly driven by redox changes in the hypolimnion and related diagenetic processes in surface sediments instead of driven by terrestrial inputs (Boyle, 2001; Naeher et al., 2013). In Lake Burgäschi, in Zone I to III, Mn and Fe varied mostly independently of erosion indicators as shown in Fig. S7b. Furthermore, Van Raden (2012) has revealed that the presence of Mn-rich laminae in sediments of Lake Burgäschi can indicate frequent short-term wind-induced mixing events in the lake. Therefore, we suggest that the deposition of Fe and Mn during these three zones was mainly controlled by in-lake processes. The proxy of XRF-inferred Fe/Mn ratios together with Mn precipitation in sediments reliably tracks past changes of hypolimnetic oxygenation of Lake Burgäschi.

In Zone I (pre ~1926), the sediments feature well-preserved Mn-Fe rich laminations and very low Fe/Mn ratios (Fig. 3 and 4a), suggesting that the lake hypolimnion was seasonally well-oxygenated. The similar occurrence of visible Mn-and Fe rich laminae in sediments were also reported by Rey et al. (2017) in Lake Burgäschi and from other lakes, for example, Lake of the Clouds in the US (Anthony, 1977), Lake Cadagno in the Swiss Alps (Wirth et al., 2013), and Lake Żabińskie in Poland (Żarczyński et al., 2018). They revealed that the red-orange Mn-rich layers mostly consist of authigenic rhodochrosite ($MnCO_3$) that was formed when Mn-rich anoxic bottom waters are mixed with oxygenated surface waters for short intervals. The preservation of this Mn-rich layer is only possible when its sedimentation process exceeds the release process under anoxic hypolimnetic conditions (Stevens et al., 2000). Therefore, during this period, short-term mixing events and associated oxygenation may have occurred during overall stratified or anoxic conditions in the hypolimnion.

In Zone II (~1926-1960), the higher Fe/Mn ratios and very low Mn- and autochthonous Fe (Fe/Ti) amounts are interpreted as the results of stable anoxic hypolimnetic waters. The formation and preservation of Fe-and Mn-oxides in sediments is largely prevented under long-term stratification/reducing conditions (Stevens et al., 2000). The lake most likely developed anoxic hypolimnetic conditions with yearly incomplete or missing circulation in the hypolimnion.

In Zone III (1960-1977), overall decreased Fe/Mn ratios combined with reappearing Mn-and Fe-rich laminations reflect better short-term oxic conditions in hypolimnetic waters than in Zone II. However, during ~1970 to 1977, Fe/Mn ratios gradually increased (Fig. 3), which points to less oxic conditions in the hypolimnion. It seems to be related to synchronously progressive lake eutrophication (see Sect. 5.1). Higher primary productivity and strengthened anoxia in the hypolimnion are commonly observed in stratified lakes (Giguet-Covex et al., 2010; Mikomägi et al., 2016). Higher lake primary productivity increases high-rate aerobic degradation of organic matter and, consequently, oxygen-depletion in the hypolimnion and sediments (Gächter and Müller, 2003; Nürnberg, 2007).

378

379   Finally, in Zone IV (1977- 2017) Fe/Mn ratios proxy is no longer valid to indicate hypolimnetic oxygenation

380   regime, as suggested by predominantly terrestrial sources of sediment Fe and Mn (Fig. S7b). Nevertheless, the

381   well-preserved laminated sediments during this period are a clear sign of absent benthic bioturbation and thus

382   represent an indicator of generally strong anoxic conditions in hypolimnetic waters, occurring simultaneously with

383   a highly eutrophic period. According to the limnological monitoring data of Lake Burgäschi between 1978 and

384   2007 (GSA, 2007), the lake water was anoxic at depths below 20 m during the summer-autumn stratification; even

385   during winter overturn of most years, the lake water was not completely mixed.

386

387   **5.3 Phosphorus composition and factors controlling long-term P-fraction retention in sediments**

388   Prior to 1977 (i.e. Zones I-III), NaBD-TP (redox-sensitive Fe- and Mn bound P) and NaOH-TP (partly non-

389   reducible Fe oxides-P) fractions were the primary P forms in sediments of Lake Burgäschi (Fig. 6 and 8). This

390   seems to compare well with the study of Moosmann et al. (2006), who suggested that sediment Fe contents control

391   P retention in sediments of the Swiss Plateau lakes. However, after ~1977, we observed a change to predominantly

392   Ca-P (apatite-P), occurring concurrently with the operation of hypolimnetic withdrawal restoration. This clear

393   pattern in sedimentary P-fraction change can be largely attributed to this restoration measure. The hypolimnetic

394   withdrawal treatment in Lake Burgäschi removes not only hypolimnetic P but also dissolved metal (Al, Fe and

395   Mn) ions and, thus leads to calcite as the main sorbent for P in upper waters and to an enhanced proportion of Ca-

396   P fraction in sediments.

397

398   In spite of the effects of lake restoration on sedimentary P retention in Zone IV, overall, the retention of total P

399   and labile P fractions in the sediment profile was mainly controlled by autochthonous Fe (Fe/Ti), Mn, and

400   hypolimnetic oxygenation proxy-Fe/Mn ratios, as shown by the results of RDA analysis (Fig. 7). Our results

401   support the previous suggestion that long-term permanent sediment-P retention is largely limited by the sediment's

402   binding capacity in anoxic conditions (Moosmann et al., 2006; Hupfer and Lewandowski, 2008), which,

403   specifically in our case, is determined by redox-sensitive elements (autochthonous Fe and Mn) preserved in

404   sediments. These findings are discussed in the context of each cluster zone as follows: During Zone I and Zone

405   III, when the hypolimnion had better seasonally oxic conditions (see Fig. 8 and Fig. S11), the increased retention

406   of Mn and Fe, and labile P fractions occurred simultaneously (Fig. 3 and 5). This phenomenon might be caused

407   by efficient P-trapping in Mn- and Fe enriched layers. It has been suggested that the formation of laminated Mn-

408   and Fe enriched layers could serve as a protective cap to reduce P release from surface sediment layers to the

409   anoxic hypolimnion (Żarczyński et al., 2018) which, thus, can help improve P retention within these sedimentary

410   layers. In Zone II, small amounts of labile P fractions might result from decreased P-bearing solid phases (Mn and

411   Fe minerals) in sediments under anoxic conditions in the hypolimnion (see higher Fe/Mn ratios in Sect. 5.2; Fig.

412   S11). However, in Zone IV, we observed the lowest retention and NBR of total P and labile P fractions in recent

413   sediments (Fig. 5; Fig. S9). We interpret this as a combined result of eutrophication-induced hypolimnetic anoxia

414   and hypolimnetic withdrawal since 1977 whereby P-rich hypolimnetic water is discharged out of the lake. On the

415   one hand, under stable anoxic conditions in the hypolimnion caused by strong eutrophication, reduced Mn and Fe

416   preservation (Fig. 3) suggests a low capacity of permanent P-trapping within the anoxic sediments. On the other

hand, hypolimnetic withdrawal restoration in Lake Burgäschi has substantially reduced hypolimnetic P concentrations by a factor of 5-6 since 1978 (Fig. S11; GSA, 2007) and MARs (Fig. 2c and Fig. S9). This indicates a concomitant decrease in sediment-P release to the hypolimnion and P sedimentation to the water-sediment interface (gross sedimentation of P) as well. Consequently, decreased total P concentrations and total P-NBR in sediments were observed (Fig. 6a and S9). The reduction of total P contents in upper sediments caused by hypolimnetic withdrawal was also reported from Lake Kortowskie of Poland (Dunalska et al., 2007). Moreover, our findings confirm that this restoration is an effective method to reduce sediment-P release potentials, as indicated by considerably decreased NBR of labile P fractions in upper sediments (Fig. S9).

In the whole sediment profile, HCl-P and Ref.-P_o fractions had mainly autochthonous origins and were mainly controlled by in-lake processes rather than by clastic inputs (e.g. apart from molasses sandstone), as indicated by absent positive correlations between the two fractions and detrital elements such as Ti, K and Al (Fig. 7). HCl-P (i.e. Ca-P) fraction retention, to a large extent, resulted from authigenic $CaCO_3$-P precipitation, and increased with higher eutrophic levels in Zone III and IV (Fig. 5; Sect. 5.1). We interpret this as an incidence of biologically driven co-precipitation of Ca and P in highly productive lakes. The phenomenon of Ca-P co-precipitation has been observed and studied in many calcareous lakes (Dittrich and Koschel 2002; Whitehouse, 2010), and is assumed to be responsible for the scavenging of dissolved P from surface waters of eutrophic lakes (Hamilton et al., 2009). In addition, large amounts of Ca-P in surface sediments (top 21 cm) can act as a potential negative feedback to eutrophication in Lake Burgäschi, because Ca-P fraction is relatively stable in sediments and has low potentials of P-release from surface sediments back to lake waters. Interestingly, HCl-P fraction retention and NBR in sediments of Zone IV were generally lower than in Zone III (Fig. 5 and Fig. S9), although the lake in Zone IV had relatively higher eutrophic levels (see Sect. 5.1; Fig. S11). The pH in the hypolimnion of Lake Burgäschi varied between 7.0 and 7.5 according to the monitoring data in 1993, 2003, and 2013 (Guthruf et al., 2013). Therefore, the acid dissolution of Ca-P in the hypolimnion and at the water-sediment interface is small and unlikely significant during Zone IV. The generally decreased retention and NBR of Ca-P fraction were seemingly related to hypolimnetic withdrawal, which has caused lower water-P concentrations and MAR of sediments as discussed above. As a result, there are reductions of $CaCO_3$-P co-precipitation in the epilimnion and consequently of Ca-P net sedimentation in surface sediments. Overall, Ref.-P_o fraction retention and NBR in the sedimentary profile show less variability compared with other P fractions (Fig. 5 and Fig. S9). Nevertheless, the lower NBR of Ref.-P_o fraction in the upper sediments (~ top 10 cm) could be derived from the ongoing early degradation of fresh organic matters.

The interesting observation is that the water-P reductions caused by the hypolimnetic withdrawal in Lake Burgäschi (GSA, 2007; Nürnberg, 2007) have been ineffective in reducing algal blooms and curbing eutrophication. Similar findings were also reported from some lakes in Europe and the US (Kosten et al., 2012; Kolzau et al., 2014; Fastner et al., 2016). These authors have attributed this phenomenon to insufficient external P-load reduction, higher water temperatures under global warming of the last few decades, and the light or nitrogen limitation of surface-water phytoplankton. In Lake Burgäschi, phytoplankton growth in the trophic zone is more likely limited by P during growth season after 1978 rather than by the nitrogen (GSA, 2007) as the algae-available ortho-phosphate is almost completely used up in the epilimnion when the nitrate concentrations stay as high as 0.5-3 mg N / L in the upper 5-m waters (GBL, 1995). Hence, we suggest that these factors mentioned above,

457 except for nitrogen limitation of lake productivity, may also contribute to promoting persistently high primary

458 productivity in Lake Burgäschi. But the main driver keeping productivity high, is the continuing high external P

459 loads from the lake catchment. During summer stratification, the high lake external P load into the epilimnion

460 primarily supports phytoplankton growth in the photic zone, which is not strongly influenced by the hypolimnetic-

461 P discharge and internal P loadings. From a management perspective, it is still critically important to focus on

462 lowering external P loads in order to decrease primary production and eutrophication in seasonally-stratified small

463 deep lakes which are more likely to favor stable stratification during phytoplankton growth season.

464

465 **6 Conclusion**

466 This study shows that in Lake Burgäschi, more than half of sediment P is buried in relatively labile P fractions

467 (Fe/Mn/Al-P), yet with low potentials for P-release from these labile P fractions in deeper layers (below ~21 cm).

468 Our results highlight the importance of hypolimnetic oxygenation/mixing regime in controlling long-term P

469 retention and net burial rates of labile P fractions in sediments of this small deep lake. Irrespective of increasing

470 lake primary productivity during early 1900s to 1977, the two periods of high sedimentary retention of total P and

471 labile P-fraction occurred in Fe- and Mn enriched laminae, which appears to be linked to seasonal mixing of the

472 hypolimnion in the past. Importantly, the positive effects of hypolimnetic withdrawal in Lake Burgäschi were

473 observed primarily in sediment P-fraction data but not in lake trophic state. The 40-year operation of hypolimnetic

474 withdrawal has impoverished sedimentary P, in particular largely decreased net burial rates of labile P fractions

475 (potential internal P loads), and increased the relative proportion of stable Ca-P fraction in top sediment layers (0-

476 21 cm). Nevertheless, the lake is currently still highly eutrophic. We attribute the delay of lake recovery primarily

477 to still high nutrient inputs from the nearby or surrounding agricultural area into the lake trophic zone during

478 stratification seasons. This study calls for consistently more effective measures to minimize external P loadings

479 from the catchment, such as optimizing fertilizer application practices and technical measures in the drainages.

480

481

482

483 **Data availability**

484 The data is available at PANGAEA at https://doi.org/10.1594/PANGAEA.908896.

485

486

487 **Author contributions**

488 L.T. helped with sample collection, analyzed the sediment, conducted data analysis, wrote the manuscript, and

489 acquired most of the funding for the project.

490 P. Z. helped with sediment core subsampling, conducted the hyperspectral imaging (HSI) scanning, helped with

491 XRF-scanning, substantially contributed to the data interpretation.

492 S.S. measured gamma-spectroscopy radiometric activities, generated the data for chronology and helped with

493 data interpretation.

494 R.L. conducted the XRF-scanning and helped with data interpretation.

495 M.G. designed the study, helped discussing the results, editing the manuscript and supervised the project.

496 All authors commented on the manuscript.

497

Competing interests

The authors declare that they have no conflict of interest.

Acknowledgements

We thank Stamatina Makri and Dr. Andre F. Lotter for their help during the fieldwork. We thank Irene Brunner, Patrick Neuhaus, Dr. Daniela Fischer and Andrea Sanchini for their expertise and the lab assistance. Further, we acknowledge Dr. Klaus A. Jarosch for the valuable suggestions about phosphorus data. The thoughtful comments and suggestion by the two anonymous reviewers greatly improved this paper. The project was funded by the Swiss National Science Foundation under the grant number 200021-172586, a Fellowship Grant from the Chinese Scholarship Counsel and the International PhD Fellowship from University of Bern.

508

509

References

Anthony, R. S.: Iron-rich rhythmically laminated sediments in Lake of the Clouds, northeastern Minnesota, Limnol. Oceanogr., 22, 45–54, https://doi.org/10.4319/lo.1977.22.1.0045, 1977.

Appleby, P.G.: Chronostratigraphic techniques in recent sediments, In: Tracking Environmental Change Using Lake Sediments. Basin Analysis, Coring, and Chronological Techniques, edited by: Last, W.M., and Smol, J.P., Springer, Dordrecht, Netherlands, 171-203, https://doi.org/10.1007/0-306-47669-X_9, 2002.

Bennett, K. D.: Determination of the number of zones in a biostratigraphical sequence, New Phytol., 132, 155–170, https://doi.org/10.1111/j.1469-8137.1996.tb04521.x, 1996.

Binderheim-Bankay, E. A.: Sanierungsziel für natürlich eutrophe Kleinseen des Schweizer Mittellandes, Ph.D. thesis, ETH Zurich, Switzerland, 149 pp., 1998.

Bonk, A., Kinder, M., Enters, D., Grosjean, M., Meyer-Jacob, C., and Tylmann, W.: Sedimentological and geochemical responses of Lake Żabińskie (north-eastern Poland) to erosion changes during the last millennium, J. Paleolimnol., 56, 239–252, https://doi.org/10.1007/s10933-016-9910-6, 2016.

Boyle, J. F.: Inorganic Geochemical Methods in Palaeolimnology, In: Tracking Environmental Change Using Lake Sediments. Basin Analysis, Coring, and Chronological Techniques, edited by: Last, W.M., and Smol, J.P., Springer, Dordrecht, Netherlands, 83-141, https://doi.org/10.1007/0-306-47670-3_5, 2002.

Büren, G. von: Der Burgäschisee, Mitteilungen der Naturforschenden Gesellschaft, Bern, 83 pp.,1949.

Burley, K.L., Prepas, E.E., and Chambers, P.A.: Phosphorus release from sediments in hardwater eutrophic lakes: the effects of redox-sensitive and-insensitive chemical treatments, Freshwater Biol., 46, 1061–1074, https://doi.org/10.1046/j.1365-2427.2001.00789.x, 2001.

Butz, C., Grosjean, M., Fischer, D., Wunderle, S., Tylmann, W., and Rein, B.: Hyperspectral imaging spectroscopy: a promising method for the biogeochemical analysis of lake sediments, J. Appl. Remote Sens., 9, 1–20, https://doi.org/10.1117/1.JRS.9.096031, 2015.

Butz, C., Grosjean, M., Goslar, T., and Tylmann, W.: Hyperspectral imaging of sedimentary bacterial pigments: a 1700-year history of meromixis from varved Lake Jaczno, northeast Poland, J. Paleolimnol., 58, 57–72,

https://doi.org/10.1007/s10933-017-9955-1, 2017.

Cavalcante, H., Araujo, F. Noyma, N.P., and Becker, V.: Phosphorus fractionation in sediments of tropical semiarid reservoirs. Sci. Total Environ., 619-620, 1022–1029, https://doi.org/10.1016/j.scitotenv.2017.11.204, 2018

Chen, M., Ding, S., Chen, X., Sun, Q., Fan, X., Lin, J., Ren, M., Yang, L., and Zhang, C.: Mechanisms driving phosphorus release during algal blooms based on hourly changes in iron and phosphorus concentrations in sediments, Water res., 133, 153–164. https://doi.org/10.1016/j.watres.2018.01.040, 2018.

Dittrich, M. and Koschel, R.: Interactions between calcite precipitation (natural and artificial) and phosphorus cycle in the hardwater lake, Hydrobiologia, 469, 49–57, https://doi.org/10.1023/A:1015571410442, 2002.

Dunalska, J.A., Wiśniewski, G., and Mientki, C.: Assessment of multi-year (1956-2003) hypolimnetic withdrawal from Lake Kortowskie, Poland, Lake and Reserv. Manage., 23, 377-387, https://doi.org/10.1080/07438140709354025, 2007.

Einsele, W.: Über die Beziehungen des Eisenkreislaufs zum Phosphatkreislauf im eutrophen See, Arch. Hydrobiol., 29, 664–686, 1936.

Einsele, W.: Über chemische und kolloidchemische Vorgänge in Eisen-Phosphat- Systemen unter limnischen und limnogeologischen Gesichtpunkten, Arch. Hydrobiol., 33, 361–387, 1938.

Enters, D., Lücke, A., and Zolitschka, B.: Effects of land-use change on deposition and composition of organic matter in Frickenhauser See, northern Bavaria, Germany, Sci. Total Environ., 369, 178–187, https://doi.org/10.1016/j.scitotenv.2006.05.020, 2006.

Fastner, J., Abella, S., Litt, A., Morabito, G., Vörös, L., Pálffy, K., Straile, D., Kümmerlin, R., Matthews, D., Phillips, M.G., and Chorus, I.: Combating cyanobacterial proliferation by avoiding or treating inflows with high P load—experiences from eight case studies, Aquat. Ecol., 50, 367–383, https://doi.org/10.1007/s10452-015-9558-8, 2016.

Frugone-Álvarez, M., Latorre, C., Giralt, S., Polanco-Martínez, J., Bernárdez, P., Oliva-Urcia, B., Maldonado, A., Carrevedo, M.L., Moreno, A., Delgado Huertas, A., and Prego, R.: A 7000-year high-resolution lake sediment record from coastal central Chile (Lago Vichuquén, 34° S): implications for past sea level and environmental variability, J. Quaternary Sci., 32, 830–844, https://doi.org/10.1002/jqs.2936, 2017.

Gächter, R.: Die Tiefenwasserableitung, ein Weg zur Sanierung von Seen, Schweizerische Zeitschrift für Hydrologie, 38, 1–28, 1976.

Gächter, R.: Lake restoration. Why oxygenation and artificial mixing cannot substitute for a decrease in the external phosphorus loading, Aquat. Sci., 49, 176–185, https://doi.org/10.1007/BF02538501, 1987.

Gächter, R. and Wehrli, B.: Ten years of artificial mixing and oxygenation: no effect on the internal phosphorus loading of two eutrophic lakes, Environ. Sci. Technol., 32, 3659–3665, https://doi.org/10.1021/es980418, 1998.

Gächter, R. and Müller, B.: Why the phosphorus retention of lakes does not necessarily depend on the oxygen supply to their sediment surface, Limnol. Oceanogr., 48, 929–933, https://doi.org/10.4319/lo.2003.48.2.0929, 2003.

Giguet-Covex, C., Arnaud, F., Poulenard, J., Enters, D., Reyss, J.L., Millet, L., Lazzaroto, J., and Vidal, O.: Sedimentological and geochemical records of past trophic state and hypolimnetic anoxia in large, hard-water Lake Bourget, French Alps, J. Paleolimnol., 43, 171–190, https://doi.org/10.1007/s10933-009-9324-9, 2010.

574 Gonsiorczyk, T., Casper, P., and Koschel, R.: Phosphorus-binding forms in the sediment of an oligotrophic and an
575 eutrophic hardwater lake of the Baltic Lake District (Germany), Water Sci. Technol., 37, 51–58,
576 https://doi.org/10.1016/S0273-1223(98)00055-9, 1998.

577 Grimm, E. C.: CONISS: a FORTRAN 77 program for stratigraphically constrained cluster analysis by the method
578 of incremental sum of squares, Comput. Geosci., 13,13–35, https://doi.org/10.1016/0098-3004(87)90022-7, 1987.

579 Guthruf, J., Zeh, M., and Guthruf-Seiler, K.: Kleinseen im Kanton Bern, Water Protection and Waste Management
580 Office of the Canton of Bern, Bern, 1999.

581 Guthruf, K., Maurer, V., Ryser, R., Zeh, M., and Zweifel, N.: Zustand der Kleinseen, Construction, Transport and
582 Energy Directorate of the Canton of Bern Office for Water and Waste Water and soil protection laboratory, Bern,
583 2013.

584 Håkanson, L. and Jansson, M. (Eds.) : Principles of Lake Sedimentology, The Blackburn Press, New Jersey, USA,
585 2002.

586 Hamilton, S.K., Bruesewitz, D.A., Horst, G.P., Weed, D.B., and Sarnelle, O.: Biogenic calcite–phosphorus
587 precipitation as a negative feedback to lake eutrophication, Can. J. Fish. Aquat. Sci., 66, 343–
588 350, https://doi.org/10.1139/F09-003, 2009.

589 Heiri, O., Lotter, A. F., and Lemcke, G.: Loss on ignition as a method for estimating organic and carbonate content
590 in sediments: reproducibility and comparability of results, J. Paleolimnol., 25, 101–110,
591 https://doi.org/10.1023/A:1008119611481, 2001.

592 Holmer, M. and Storkholm, P.: Sulphate reduction and sulphur cycling in lake sediments: a review, Freshwater
593 Biol., 46, 431–451, https://doi.org/10.1046/j.1365-2427.2001.00687.x, 2001.

594 Hupfer, M. and Lewandowski, J.: Oxygen controls the phosphorus release from lake sediments–a long-lasting
595 paradigm in limnology, Int. Rev. Hydrobiol., 93, 415–432, https://doi.org/10.1002/iroh.200711054, 2008.

596 Juggins, S.: rioja: analysis of quaternary science data, https://cran.r-project.org/web/packages/rioja/index.html,
597 2017.

598 Kaiserli, A., Voutsa, D., and Samara, C.: Phosphorus fractionation in lake sediments–lakes Volvi and Koronia,
599 N. Greece, Chemosphere, 46, 1147–1155, https://doi.org/10.1016/S0045-6535(01)00242-9, 2002.

600 Kolzau, S., Wiedner, C., Rücker, J., Köhler, J., Köhler, A., and Dolman, A. M.: Seasonal patterns of nitrogen and
601 phosphorus limitation in four German lakes and the predictability of limitation status from ambient nutrient
602 concentrations, Plos One, 9, e96065, https://doi.org/10.1371/journal.pone.0096065, 2014.

603 Kosten, S., Huszar, V.L., Bécares, E., Costa, L.S., van Donk, E., Hansson, L.A., Jeppesen, E., Kruk, C., Lacerot,
604 G., Mazzeo, N., and De Meester, L.: Warmer climates boost cyanobacterial dominance in shallow lakes, Global,
605 Change Biol., 18, 118–126, https://doi.org/10.1111/j.1365-2486.2011.02488.x, 2012.

606 Kucklentz, V. and Hamm, A. (Eds.): Möglichkeiten und Erfolgsaussichten der Seenrestaurierung, Bayrische
607 Landesanstalt für Wasserforschung, München, Germany, 212 pp., 1988.

608 LAWA (Länderarbeitsgemeinschaft Wasser): Gewässerbewertung — stehende Gewässer: Richtlinie für die
609 Bewertung nach trophischen Kriterien, Germany, 1998.

610 Lukkari, K., Hartikainen, H., and Leivuori, M.: Fractionation of sediment phosphorus revisited. I: Fractionation
611 steps and their biogeochemical basis, Limnol. Oceanog- Meth., 5, 433–444,
612 https://doi.org/10.4319/lom.2007.5.433, 2007.

613 Mackereth, F.J.H.: Some chemical observations on post-glacial lake sediments, Philos. T. Roy. Soc. B., 250, 165–
614 213, https://doi.org/10.1098/rstb.1966.0001, 1966.

615 GBL. Burgäschisee. Resultate der Wasser- und Planktonuntersuchungen 1977-1995. Office for Water Protection
616 and Waste Management of the Canton of Bern, 1995.

617 GSA: 30 Jahre Tiefenwasser-Ableitung. Wie geht es dem Burgäschisee heute?, Office for Water Protection and
618 Waste Management of the Canton of Bern, Bern, 2007.

619 McCulloch, J., Gudimov, A. Arhonditsis,G. Chesnyuk, A., and Dittrich, M.: Dynamics of P-binding forms in
620 sediments of a mesotrophic hard-water lake: Insights from non-steady state reactive-transport modeling, sensitivity
621 and identifiability analysis, Chem. Geol., 354, 216–232, https://doi.org/10.1016/j.chemgeo.2013.06.011, 2013.

622 Meyers, P. A. and Ishiwatari, R.: Lacustrine organic geochemistry—an overview of indicators of organic matter
623 sources and diagenesis in lake sediments, Org. Geochem., 20, 867–900, http://dx.doi.org/10.1016/0146-
624 6380(93)90100-P, 1993,

625 Michel, H., Barci-Funel, G., Dalmasso, J., Ardisson, G., Appleby, P., Haworth, E., and El-Daoushy, F.: Plutonium,
626 americium and cesium records in sediment cores from Blelham Tarn, Cumbria (UK), J. Radioanal. Nucl. Ch., 247,
627 107–110, https://doi.org/10.1023/A:1006719215833, 2001.

628 Moosmann, L., Gächter, R. Müller, B., and Wüest, A.: Is phosphorus retention in autochthonous lake sediments
629 controlled by oxygen or phosphorus?, Limnol. Oceanogr., 51, 763–771,
630 https://doi.org/10.4319/lo.2006.51.1_part_2.0763, 2006.

631 Mikomägi, A., Koff, T., Martma, T., and Marzecová, A.: Biological and geochemical records of human-induced
632 eutrophication in a small hard-water lake, Boreal Env. Res., 21, 513–527, 2016.

633 Naeher, S., Gilli, A., North, R.P., Hamann, Y., and Schubert, C.J.: Tracing bottom water oxygenation with
634 sedimentary Mn/Fe ratios in Lake Zurich, Switzerland, Chem. Geol., 352, 125–133,
635 https://doi.org/10.1016/j.chemgeo.2013.06.006, 2013.

636 Nikolai, S.J. and Dzialowski, A.R.: Effects of internal phosphorus loading on nutrient limitation in a eutrophic
637 reservoir, Limnologica, 49, 33–41, https://doi.org/10.1016/j.limno.2014.08.005, 2014.

638 Nürnberg, G.K.: Lake responses to long-term hypolimnetic withdrawal treatments, Lake Reserv. Manage., 23,
639 388–409, https://doi.org/10.1080/07438140709354026, 2007.

640 Ogdahl, M. E., Steinman, A. D., and Weinert, M. E.: Laboratory-determined phosphorus flux from lake sediments
641 as a measure of internal phosphorus loading, Jove-J. Vis. Exp., 85, e51617, https://dx.doi.org/10.3791%2F51617,
642 2014.

643 Oksanen, J., Blanchet, F.G., Kindt, R., Legendre, P., Minchin, P.R., O'hara, R., Simpson, G.L., Solymos, P.,
644 Stevens, M.H.H., and Wagner, H.: Package 'vegan'. Community ecology package, version 2, http://cran.r-
645 project.org/web/packages/vegan/index.html, 2013.

646 Pennington, W., Tutin, T.G., Cambray, R.S., and Fisher, E.M.: Observations on lake sediments using fallout [137]Cs
647 as a tracer, Nature, 242, 324–326, https://doi.org/10.1038/242324a0, 1973.

648 R Development Core Team: R: A Language and Environment for Statistical Computing, R Foundation for
649 Statistical Computing, Vienna, Austria, 2017.

650 Rentz, J., Turner, I.P., and Ullman, J.L.: Removal of phosphorus from solution using biogenic iron oxides, Water
651 Res., 43, 20292035, https://doi.org/10.1016/j.watres.2009.02.021, 2009.

652 Reuss, N., Conley, D.J., and Bianchi, T.S.: Preservation conditions and the use of sediment pigments as a tool for
653 recent ecological reconstruction in four Northern European estuaries, Mar. Chem., 95, 283–302,
654 https://doi.org/10.1016/j.marchem.2004.10.002, 2005.

655 Rey, F., Gobet, E., van Leeuwen, J.F.N., Gilli, A., van Raden, U.J., Hafner, A., Wey, O., Rhiner, J., Schmocker,

656 D., Zünd, J., and Tinner, W.: Vegetational and agricultural dynamics at Burgäschisee (Swiss Plateau) recorded for

657 18,700 years by multi-proxy evidence from partly varved sediments, Veg. Hist. Archaeobot., 26, 571–586.

658 https://doi.org/10.1007/s00334-017-0635-x, 2017.

659 Ribeiro, D., Martins, G., Nogueira, R., Cruz, J.V., and Brito, A.: Phosphorus fractionation in volcanic lake

660 sediments (Azores–Portugal), Chemosphere, 70, 1256–1263, https://doi.org/10.1016/j.chemosphere.2007.07.064,

661 2008.

662 Richter, T.O., Van der Gaast, S., Koster, B., Vaars, A., Gieles, R., de Stigter, H.C., De Haas, H., and van Weering,

663 T.C.: The Avaatech XRF Core Scanner: technical description and applications to NE Atlantic sediments, Geol.

664 Soc. London Spec. Publ., 267, 39–50, https://doi.org/10.1144/GSL.SP.2006.267.01.03, 2006.

665 Rydin, E.: Potentially mobile phosphorus in Lake Erken sediment. Water Res., 34, 2037–2042,

666 https://doi.org/10.1016/S0043-1354(99)00375-9, 2000.

667 Schmid, S.M., Fügenschuh, B., Kissling, E., and Schuster, R.: Tectonic map and overall architecture of the

668 Alpine orogen, Eclogae Geol. Helv., 97, 93–117, https://doi.org/10.1007/s00015-004-1113-x, 2004.

669 Schneider, T., Rimer, D., Butz, C., and Grosjean, M.: A high-resolution pigment and productivity record from

670 the varved Ponte Tresa basin (Lake Lugano, Switzerland) since 1919: insight from an approach that combines

671 hyperspectral imaging and highperformance liquid chromatography, J. Paleolimnol., 60, 381–398,

672 https://doi.org/10.1007/s10933-018-0028-x, 2018.

673 Schnurrenberger, D., Russell, J., and Kelts, K.: Classification of lacustrine sediments based on sedimentary

674 components, J. Paleolimnol., 29,141–154, https://doi.org/10.1023/A:1023270324800, 2003.

675 Smith, L., . Watzin, M. C., and Druschel, G.: Relating sediment phosphorus mobility to seasonal and diel redox

676 fluctuations at the sediment-water interface in a eutrophic freshwater lake, Limnol. and Oceanogr., 56, 2251–

677 2264, https://doi.org/10.4319/lo.2011.56.6.2251, 2011.

678 Søndergaard, M., Jensen, P.J., and Jeppesen, E.: Retention and internal loading of phosphorus in shallow,

679 eutrophic lakes, Sci. World J., 1, 427–442, https://doi.org/10.1100/tsw.2001.72, 2001

680 Stevens, L., Ito, E., and Olson, D.: Relationship of Mn-carbonates in varved lake-sediments to catchment

681 vegetation in Big Watab Lake, MN, USA. J. Paleolimnol., 24,199–211,

682 https://doi.org/10.1023/A:1008169526577, 2000.

683 Trolle, D., Hamilton, D.P., and Pilditch, C.A.: Evaluating the influence of lakemorphology, trophic status and

684 diagenesis on geochemical profiles in lake sediments, Appl. Geochem., 25, 621–632,

685 https://doi.org/10.1016/j.apgeochem.2010.01.003, 2010.

686 Tu, L., Jarosch, K.A., Schneider, T., and Grosjean, M.: Phosphorus fractions in sediments and their relevance for

687 historical lake eutrophication in the Ponte Tresa basin (Lake Lugano, Switzerland) since 1959, Sci. Total Environ.,

688 685, 806–817, https://doi.org/10.1016/j.scitotenv.2019.06.243, 2019.

689 Tylmann, W., Bonk, A., Goslar, T., Wulf, S., and Grosjean, M.: Calibrating ^{210}Pb dating results with varve

690 chronology and independent chronostratigraphic markers: Problems and implications, Quat. Geochronol. 32, 1–

691 10, https://doi.org/10.1016/j.quageo.2015.11.004, 2016.

692 van Raden, U. J.: High-resolution Swiss lake records of climate change. Ph.D. thesis, ETH Zurich, Switzerland,

693 https://doi.org/10.3929/ethz-a-009783578, 2012.

694 Whitehouse, R.D.: Phosphorus scavenging through calcite co-precipitation: bringing clarity to Clear Lake, B.Sc.
695 thesis, University of British Columbia, Canada, 2010.

696 Wirth, S.B., Gilli, A., Niemann, H., Dahl, T.W., Ravasi, D., Sax, N., Hamann, Y., Peduzzi, R., Peduzzi, S., Tonolla,
697 M., and Lehmann, M.F.: Combining sedimentological, trace metal (Mn, Mo) and molecular evidence for
698 reconstructing past water-column redox conditions: The example of meromictic Lake Cadagno (Swiss Alps),
699 Geochim. Cosmochim. Ac., 120, 220–238, https://doi.org/10.1016/j.gca.2013.06.017, 2013.

700 Żarczyński, M., Wacnik, A., and Tylmann, W.: Tracing lake mixing and oxygenation regime using the Fe/Mn
701 ratio in varved sediments: 2000year-long record of human-induced changes from Lake Zabinskie (NE Poland),
702 Sci. Total Environ., 657, 585–596, https://doi.org/10.1016/j.scitotenv.2018.12.078, 2019.

703 Żarczyński, M., Tylmann, W., and Goslar, T.: Multiple varve chronologies for the last 2000 years from the
704 sediments of Lake Żabińskie (northeastern Poland)–Comparison of strategies for varve counting and uncertainty
705 estimations, Quaternary Geochronology, 47, 107–119, https://doi.org/10.1016/j.quageo.2018.06.001, 2018.

706
707
708
709
710
711
712
713
714
715
716
717
718
719
720
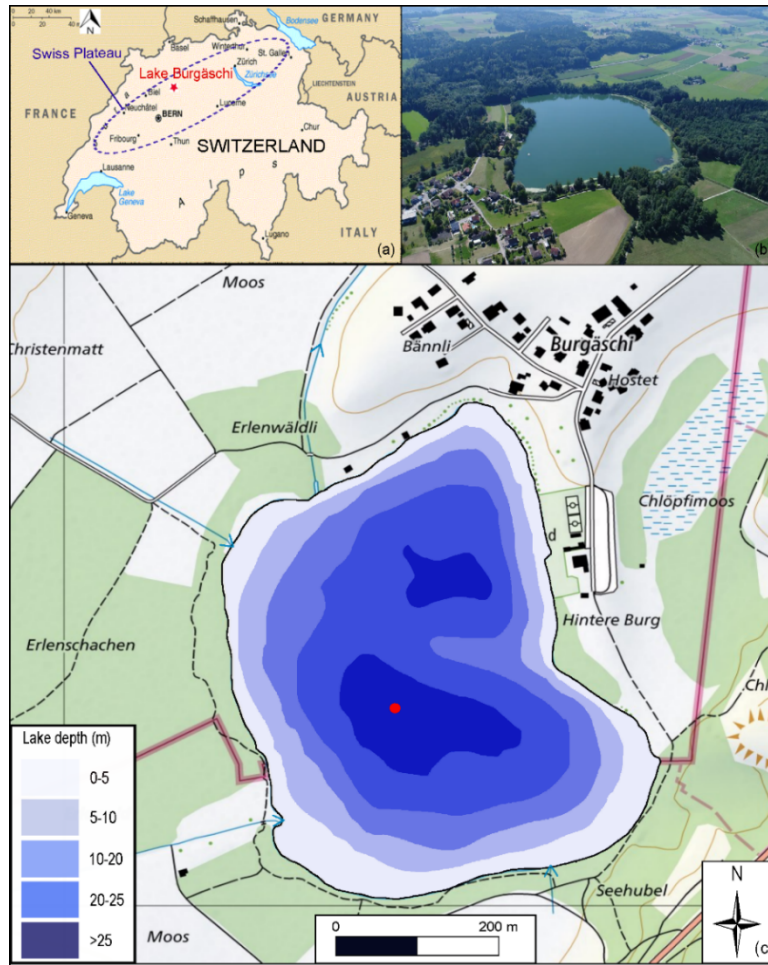
721721

722 **Figure 1: Study site. (a) Overview map of Switzerland and the Swiss Plateau. Lake Burgäschi is indicated as the red**
723 **asterisk. (b) Photo of Lake Burgäschi and catchment (© 2018 Google Maps). (c) Bathymetric map of Lake Burgäschi**
724 **adapted from Guthruf et al. (1999). The red dot indicates the coring site (color figure online). Green areas around the**
725 **lake indicate forests, white areas agricultural lands. Inflow and outflow to the lake are indicated by blue arrow lines**
726 **(topographic maps: © swisstopo).**

727

728

729

730

731

732

733

734

735

736

737

738

739

739

740

741
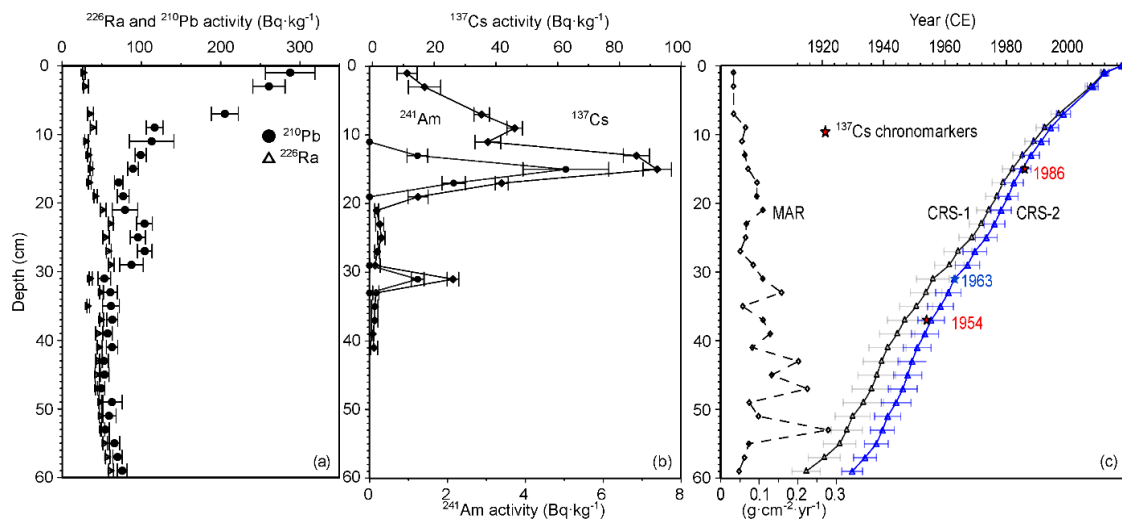
Figure 2: (a) Total ^{210}Pb, ^{226}Ra, and (b) ^{137}Cs and ^{241}Am activity concentration profiles in sediment core Burg17-B from Lake Burgäschi; (c) The comparison of different ^{210}Pb CRS models: unconstrained CRS-1 model and constrained CRS-2 model at 1963; the mass accumulation rates (MAR) are obtained from the CRS-2 model.

745

746

747

748

749
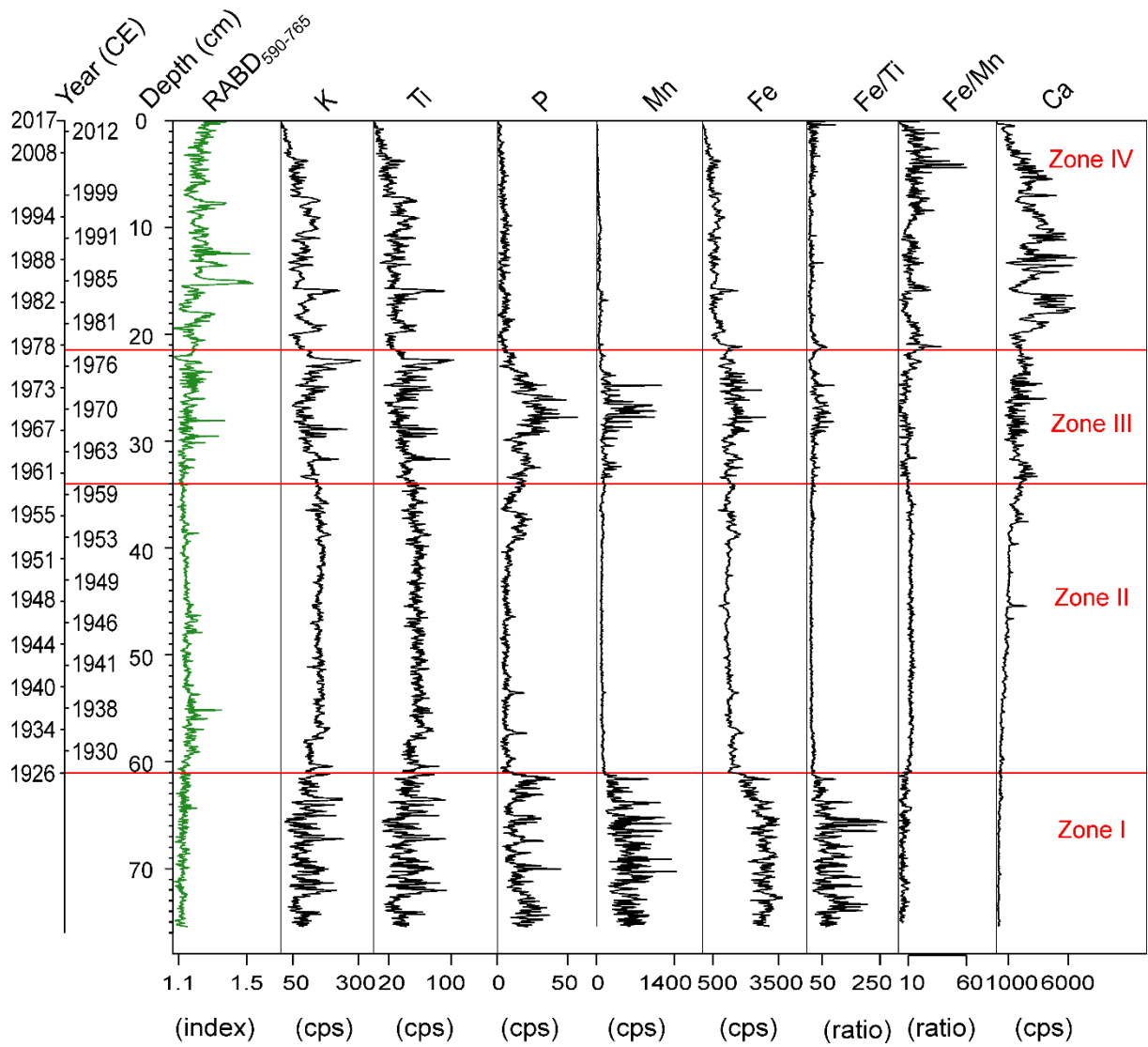
Figure 3: Stratigraphic records of HSI-inferred green-pigments (RABD$_{590-765}$) and XRF-data in sediments of core
Burg17-B. Elemental counts are represented in cps (counts per second). The red horizontal lines separate the four
significant clusters retrieved by the CONISS analysis (color figure online).
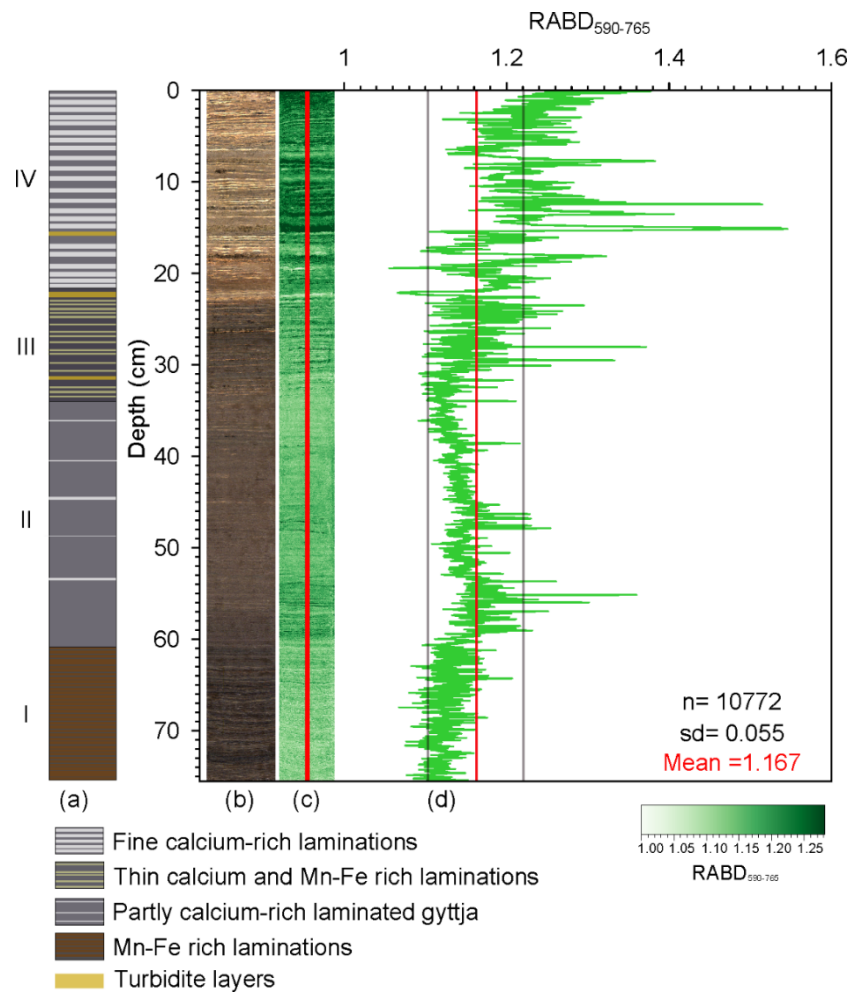
Figure 4: (a) Lithological description of Burg17-B sediment core. The intensities of Ca, Fe and Mn in each unit were inferred from XRF-element counts in Fig. 3; Yellow colors highlight the turbidite layers identified from the XRF peaks of siliciclastic elements e.g. K, Ti, and Rb. **(b)** RGB contrast enhanced sediment core picture. **(c)** The map of the spectral index $RABD_{590-765}$ (i.e. green-pigments) distribution, and **(d)** the graphic output of $RABD_{590-765}$ spectral index within the boundary of the red lines (c) which shows the 2-mm wide sampling range. The red line in (d) indicates the mean index value and the grey lines represent the one-standard deviations (sd). The colorbar represents the index values of the distribution map (color figure online). n is the number of rows of the $RABD_{590-765}$ index map.
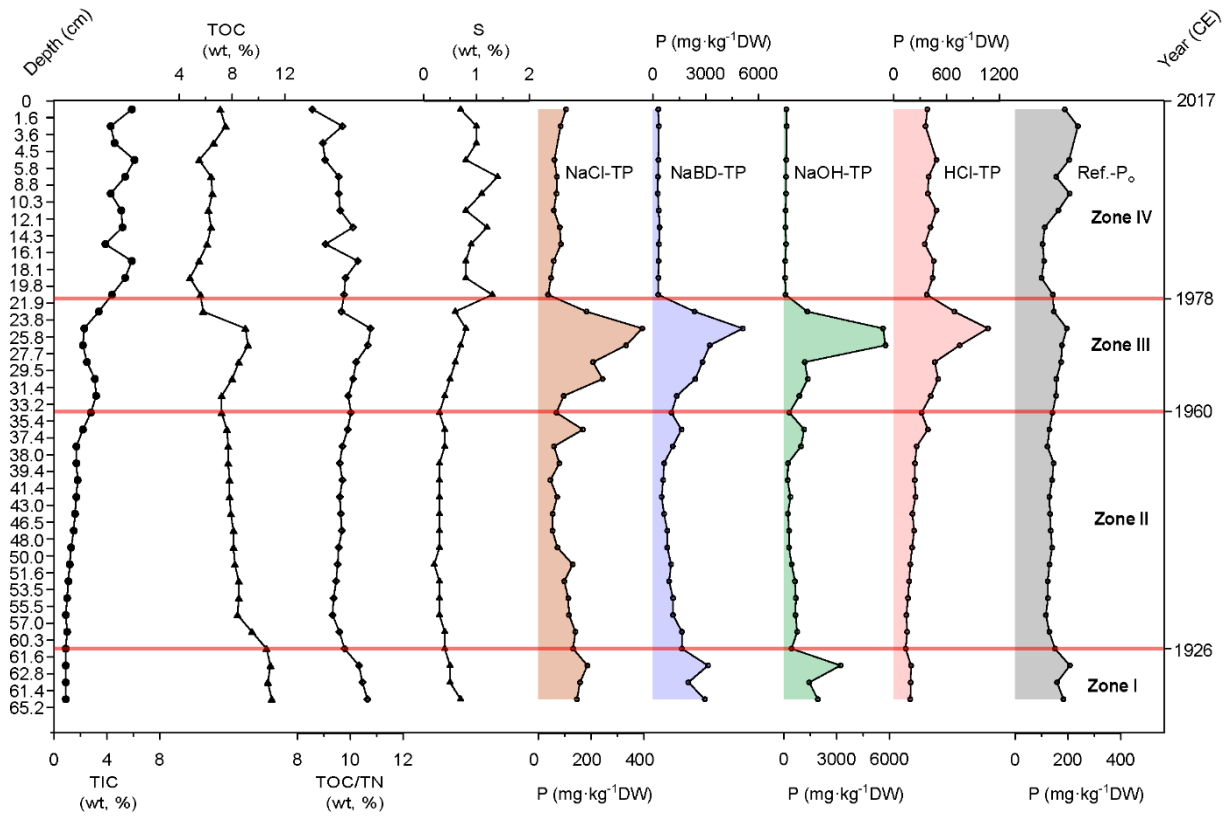
763

764 **Figure 5: The stratigraphy of total inorganic carbon (TIC), total organic carbon (TOC), sulfur (S) contents, TOC/TN**
765 **ratio and five phosphorus fractions in sediments of Lake Burgäschi. The y-axis (left) refers to the sediment depth of**
766 **core Burg17-B. The horizontal red lines separate the significant CONISS zones as in Fig. 3. The secondary y-axis (right)**
767 **indicates approximate ages of sediments inferred from the Burg17-B core chronology.**

768
769
770
771
772
773
774
775
776
777
778
779
780
781
782
783
784
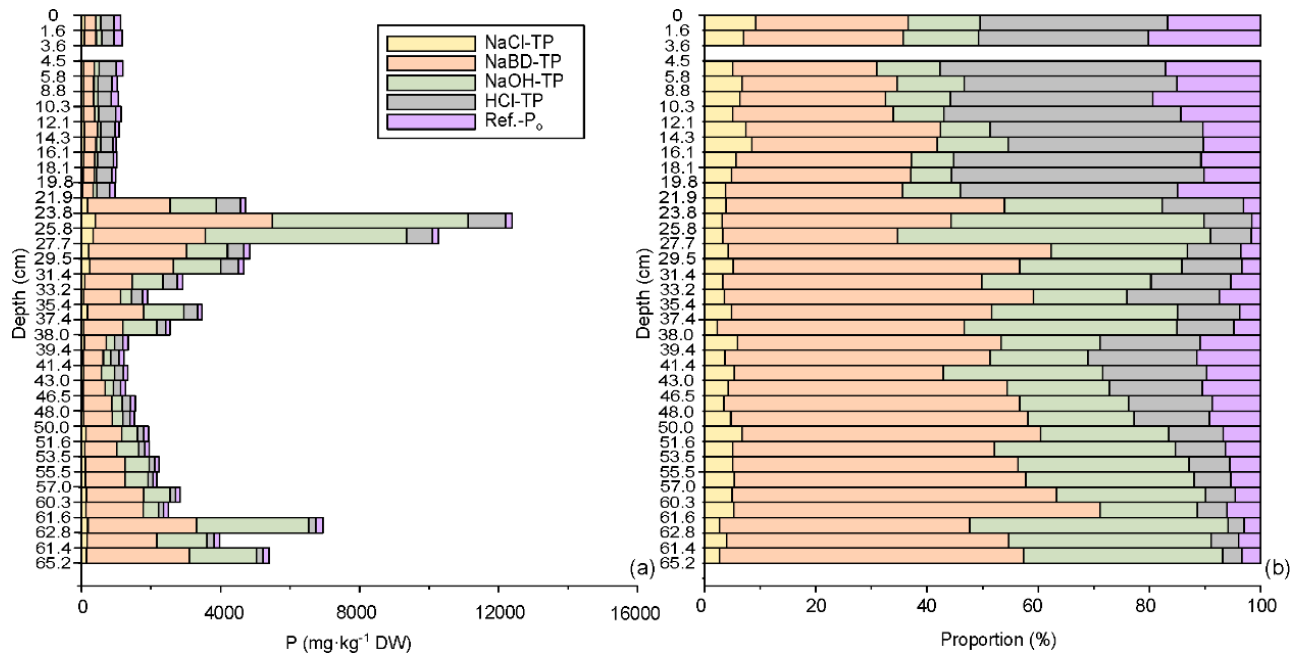
Figure 6: Vertical profile of (a) P fractions concentrations and (b) their proportions of total P in sediments. The y-axis (left) refers to the sediment depth of Core Burg17-B. Note that the sample between 3.6-4.5 cm depth was removed from dataset because the values were extremely higher than any sample data (data not shown), which is abnormal according to XRF-P counts at the corresponding depth (Fig. S8b). We attributed this to the result of contamination during the sample measurements.
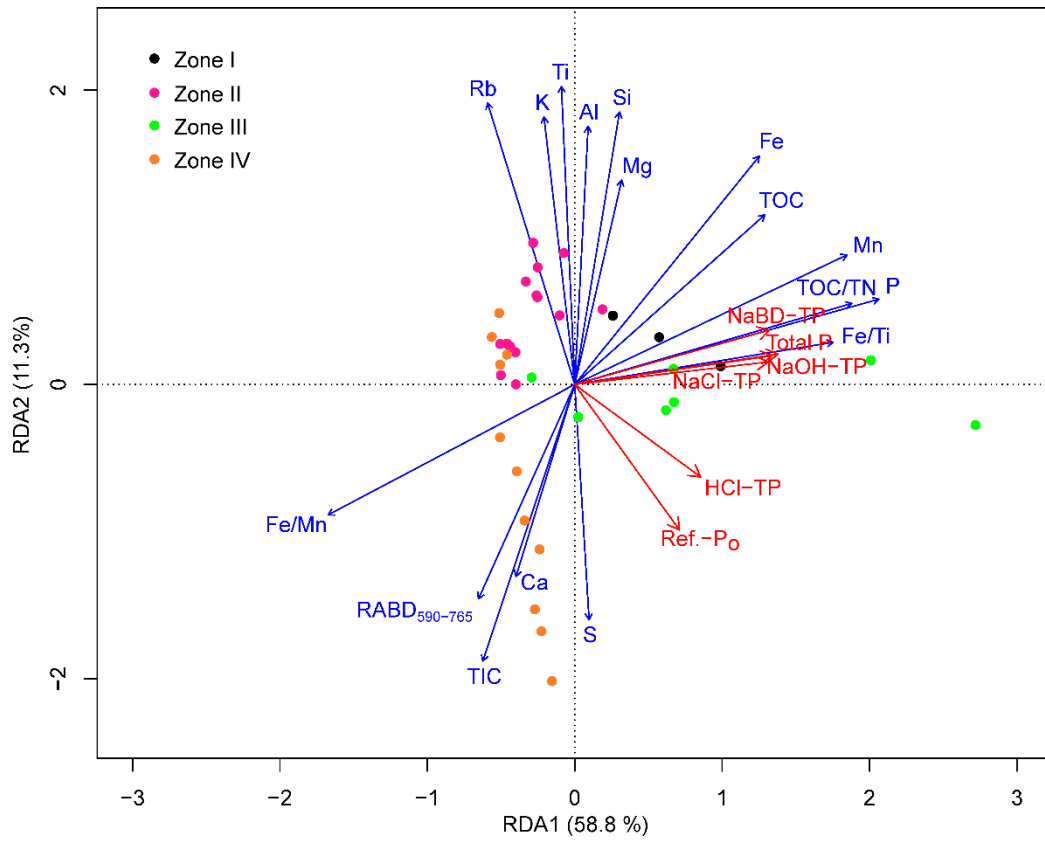
797
798

799

800 **Figure 7. RDA biplot displaying correlation between response variables (P fraction dataset; red arrows) and**
801 **explanatory variables (green-pigments and other geochemical records; blue arrows). The colored points represent data**
802 **points of individual cluster zones in Fig. 3, 5 and S6.**

803

804

805
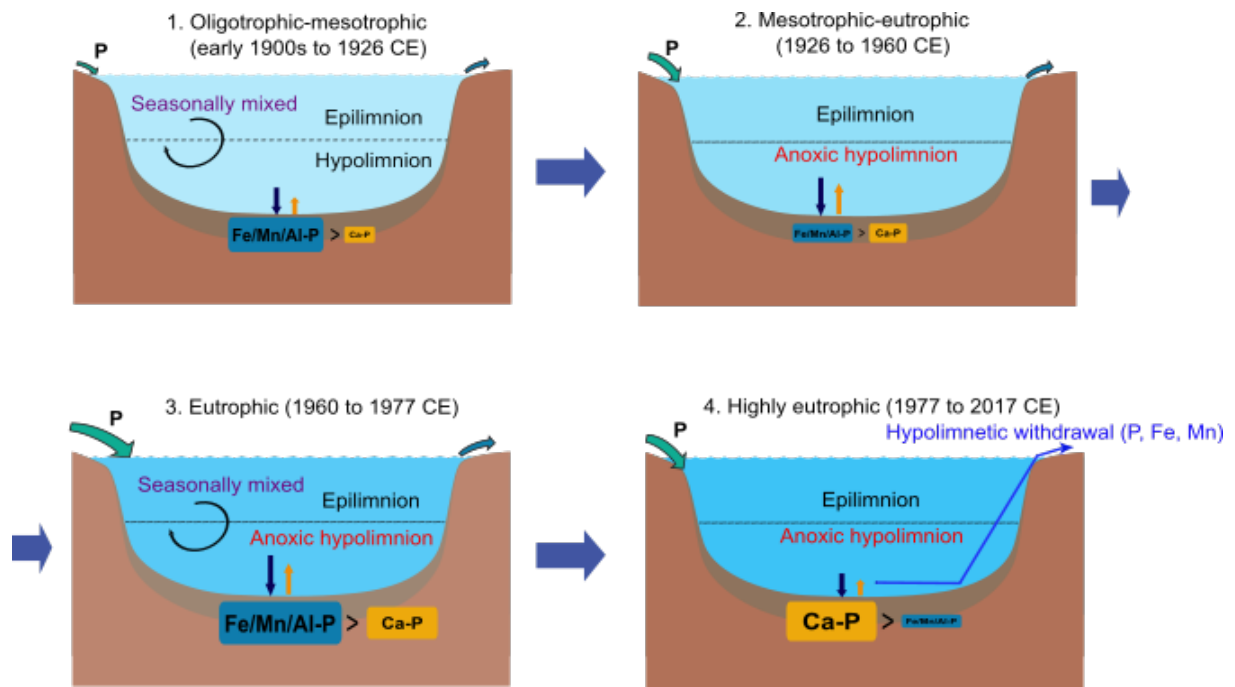
806

807

808 **Figure 8: Conceptual diagram, summarising the inputs/outputs of phosphorus (P), hypolimnetic withdrawal**
809 **restoration, lake trophic levels, mixing regime and phosphorus (P) fractions retention in sediments of Lake Burgäschi**
810 **during four stages/zones. Note that the illustrated sizes of P fractions (Fe/Mn/Al-P and Ca-P) among different stages**
811 **overall indicate the relative amounts of P fractions in sediments.**

812

813